

11-5-2001

Characterization of the native Cr_2O_3 oxide surface of CrO_2

Ruihua Cheng
University of Nebraska-Lincoln

B. Xu
University of Nebraska-Lincoln

C.N. Borca
University of Nebraska-Lincoln

Andrei Sokolov
University of Nebraska-Lincoln, sokolov@unl.edu

C.S. Yang
University of Nebraska-Lincoln

See next page for additional authors

Follow this and additional works at: <http://digitalcommons.unl.edu/physicsdowben>

 Part of the [Physics Commons](#)

Cheng, Ruihua; Xu, B.; Borca, C.N.; Sokolov, Andrei; Yang, C.S.; Yuan, Lu; Liou, Sy_Hwang; Doudin, Bernard; and Dowben, Peter A., "Characterization of the native Cr_2O_3 oxide surface of CrO_2 " (2001). *Peter Dowben Publications*. 22.
<http://digitalcommons.unl.edu/physicsdowben/22>

This Article is brought to you for free and open access by the Research Papers in Physics and Astronomy at DigitalCommons@University of Nebraska - Lincoln. It has been accepted for inclusion in Peter Dowben Publications by an authorized administrator of DigitalCommons@University of Nebraska - Lincoln.

Authors

Ruihua Cheng, B. Xu, C.N. Borca, Andrei Sokolov, C.S. Yang, Lu Yuan, Sy_Hwang Liou, Bernard Doudin, and Peter A. Dowben

Characterization of the native Cr₂O₃ oxide surface of CrO₂

Ruihua Cheng, B. Xu, C. N. Borca, A. Sokolov, C. -S. Yang, L. Yuan, S. -H. Liou, B. Doudin, and P. A. Dowben^{a)}

Department of Physics and Astronomy and the Center for Materials Research and Analysis (CMRA), Behlen Laboratory of Physics, University of Nebraska—Lincoln Lincoln, Nebraska 68588-0111

(Received 5 July 2001; accepted for publication 29 August 2001)

Using photoemission and inverse photoemission, we have been able to characterize the Cr₂O₃ oxide surface of CrO₂ thin films. The Cr₂O₃ surface oxide exhibits a band gap of about 3 eV, although the bulk CrO₂ is conducting. The thickness of this insulating Cr₂O₃ layer is twice the photoelectron escape depth which is about 2 nm thick. The effective Cr₂O₃ surface layer Debye temperature, describing motion normal to the surface, is about 370 K. From a comparison of CrO₂ films grown by different techniques, with different Cr₂O₃ content, evidence is provided that the CrO₂ may polarize the Cr₂O₃. © 2001 American Institute of Physics. [DOI: 10.1063/1.1416474]

Among the predicted half-metallic ferromagnets (metallic for one spin direction while insulating for the other spin direction, i.e., 100% spin polarization), CrO₂ routinely exhibits the highest polarization but among the lowest tunnel magnetoresistance. With half-metallic character expected on the basis of theory,^{1–6} very large tunneling magnetoresistance (TMR) is expected^{7–9} (ideally the TMR between two half-metallic ferromagnets should be infinite), but a much smaller (1%) magnetoresistance was found on CrO₂ tunnel junctions at 70 K.¹⁰ Evidence of 90% to 100% polarization has been, however, observed in spin-polarized photoemission,¹¹ vacuum tunneling,¹² and Andreev scattering.^{13–15} This work addresses the surface composition and properties of CrO₂ thin films, going beyond the simple confirmation that the stable oxide surface of CrO₂ is Cr₂O₃.¹⁶

We investigated the surfaces of CrO₂ films fabricated by two different techniques. One class of films were fabricated by laser initiated organometallic chemical vapor deposition (OMCVD),¹⁷ while the other type of films were made by rf sputtering of CrO₃ onto LaAlO₃ substrates and annealing in a high-pressure cell.¹⁸ Annealing in about 100 atm of oxygen pressure at 390 °C leads to a stable CrO₂ phase.

Prior to our studies, samples were cleaned by sputtering and annealing to remove surface contamination. From the outset, i.e., from the initial stages of surface preparation, the core level binding energies indicated that the stable surfaces were Cr₂O₃. X-ray photoemission spectroscopy (XPS) measurements were obtained using the Mg K_α line radiation (1253.6 eV) and the photoemission (UPS) measurements were acquired about normal emission angle using the He I line (21.2 eV). The inverse photoemission IPES spectra were obtained by using variable energy electrons (from 5 to 19 eV) at normal incidence and a Geiger–Muller UV photodetector. The energy resolution was ~450 meV in inverse photoemission. For both photoemission and inverse photoemission, the Fermi level was established from tantalum in electrical contact with the sample.

Figure 1 shows the room temperature normal emission

photoemission data of both the Cr 2*p* and O 1*s* core levels for both sputter deposited and laser assisted OMCVD deposited CrO₂ thin film samples. The binding energy of Cr 2*p*_{3/2} core level for the laser assisted OMCVD deposited CrO₂ thin film samples is about 576.8±0.2 eV which generally corresponds to the accepted binding energy for Cr₂O₃ oxide.¹⁹ The Cr 2*p*_{3/2} for the sputtered samples are somewhat lower, at about 576.3±0.3 eV. This suggests that the sputtered samples are more dominated by the CrO₂ oxide²⁰ in the surface region, though a shoulder at around 576.8 eV binding energy indicates the presence of some Cr₂O₃. The presence of both CrO₂ and Cr₂O₃ oxide phases in the surface region of the sputter deposited samples is more apparent in the oxygen core level spectra.

The binding energy of O 1*s* core level for OMCVD deposited sample is 531.1±0.2 eV and the spectrum for the sputtered sample also shows the peak at 531.1±0.2 eV as well as a significant shoulder around 529.5±0.2 eV. This suggests that the surfaces of both samples contain Cr₂O₃, but the Cr₂O₃ layer on the surface of sputtered films are thinner than the case for the OMCVD films. This conclusion is supported by the angle-resolved XPS (ARXPS) data in Fig. 2.

We used ARXPS to characterize the thickness of the Cr₂O₃ surface layer for the sputter deposited CrO₂ films, as has been undertaken for other oxide surfaces.²¹ The ratio of the Cr₂O₃ intensity to the CrO₂ intensity for each emission angle was derived by decomposing every O 1*s* spectrum into two peaks, corresponding to the Cr₂O₃ and CrO₂ oxide phases, respectively. This intensity ratio is shown in Fig. 2. Since the Cr₂O₃ signal increases relative to the CrO₂ signal at the higher emission angles, it is clear that Cr₂O₃ dominates the surface as the effective probing depth decreases with increasing emission angle. We find that the thickness of Cr₂O₃ layer is about twice the oxygen core level photoelectron mean free path, using a summation modeling analysis described elsewhere.²¹ This corresponds to approximately 2 nm thickness. Thus, while the x-ray diffraction data, shown as the inset in Fig. 2, is dominated by significant CrO₂ peaks, there is a small amount of the Cr₂O₃ signal, which probably has some contributions from the Cr₂O₃ surface of the sample. For the OMCVD deposited films, the Cr₂O₃ surface oxide is much thicker than the electron mean free path and therefore

^{a)}Author to whom all correspondence should be addressed at: Department of Physics and Astronomy, 255 Behlen Laboratory of Physics, University of Nebraska, Lincoln, Nebraska 68588-0111; electronic mail: pdowben@unl.edu

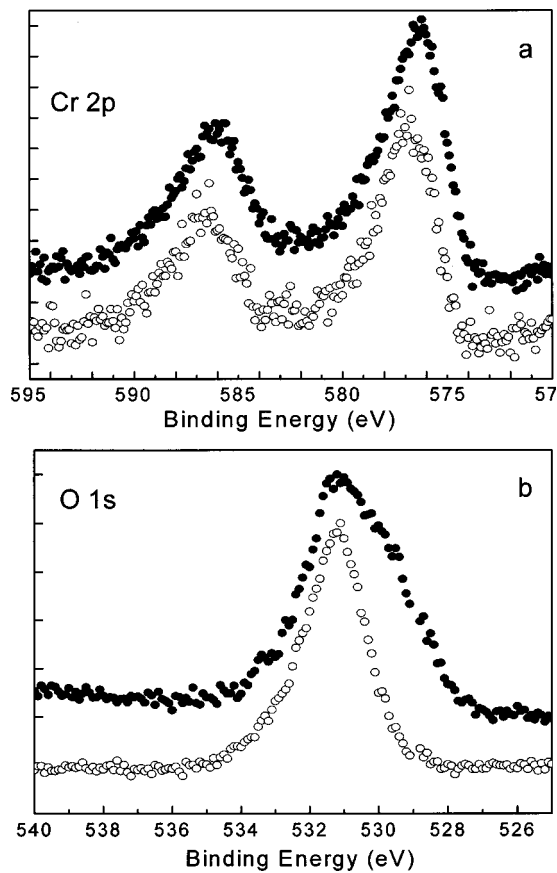


FIG. 1. Upper panel shows the XPS core level photoemission of Cr 2p at room temperature. Lower panel shows the O 1s photoemission data at room temperature. The sample fabricated by OMCVD is shown as open circles and the sample fabricated by sputtering is shown as closed circles.

is much thicker than is the case for the sputter deposited films.

The combined valence band photoemission (UPS) and inverse photoemission data taken at room temperature is shown in Fig. 3 for the sputter deposited film (curve B). A large band gap of $E_g = 2.8$ eV (at room temperature) is evident between valence band and conductance band edges. The gap is much bigger than 3 kT, which is a clear indication that the surface of CrO_2 is insulating, not conducting.

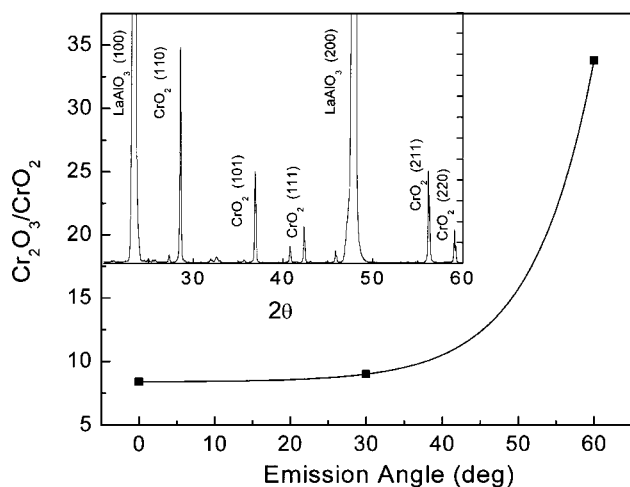


FIG. 2. The room temperature XPS intensity ratio of Cr_2O_3 peak to CrO_2 peak vs different emission angle for sputter deposited films. The x-ray diffraction data of the sample is shown in the inset.

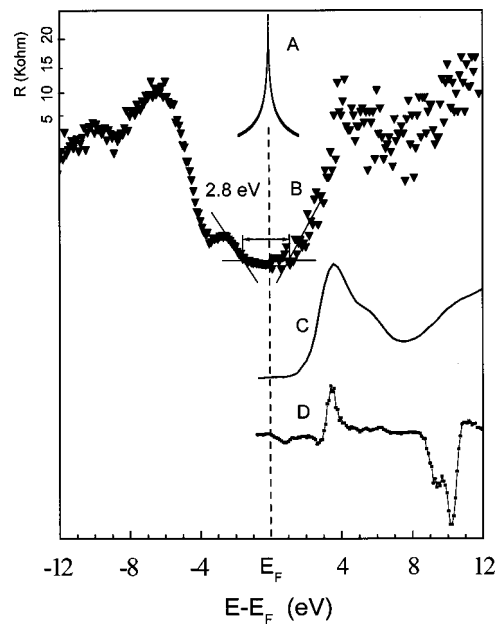


FIG. 3. A comparison of the density of states in the region of the Fermi level from resistivity (transport measurements) of the sputter deposited film at 1.52 K (a), the combined photoemission (UPS) and the inverse photoemission (IPES) at room temperature for the sputter deposited films (b), X-ray adsorption at the O 1s level (c) together with the Cr $2p_{3/2}$ edge MCD spectra (d) were both aligned using the core level binding energies for CrO_2 . Spectra C and D were taken of the OMCVD deposited sample dominated by significant amounts of Cr_2O_3 while the inverse photoemission and resistivity data were taken from a sputter deposited sample. Spectra B–D were taken at room temperature.

The transport measurements, at 1.52 K, showing the resistance at low bias voltages in the sputter deposited film, are shown in curve A of Fig. 3. At low temperatures, the resistance between CrO_2 grains in the bulk of the thin film shows a dramatic increase only near zero bias. This, together with the absence of significant surface photocharging down to 170 K, suggests that there are conduction paths through the surface region and intergrain Cr_2O_3 layers. Thus, while there is little evidence of conduction path or defects states within a volt of the Fermi level, such states must exist, though perhaps much less than 2%–3% of the Cr_2O_3 layers. This is consistent with the evidence of Coulomb blockade¹⁸ that also suggests that the Cr_2O_3 oxide surface of CrO_2 crystallites is imperfect and contains defects. For OMCVD samples, we do not find any such conducting paths, but the Cr_2O_3 content is higher in these latter films.

In Fig. 3, we lined up the chromium $L_3(2p_{3/2})$ edge magnetic circular dichroism (MCD) signal, and O 1s x-ray adsorption (XAS) spectra with the Fermi energy, based on the chromium and oxygen XPS binding energies for an OMCVD sample (characterized by significant Cr_2O_3 inclusions in the CrO_2 .¹⁷) The O 1s XAS edge spectrum (curve C in Fig. 3) is consistent with a Cr_2O_3 phase²² dominant in the surface region of the thin film material. The MCD results, shown as plot D in Fig. 3, provide indications of magnetic ordering in the unoccupied bands at the L_3 chromium edge. Nonetheless, at the onset in the MCD signal at the threshold, the magnetic ordering of the states close to the Fermi level appears to be dominated by spin minority (curve D in Fig. 3), which is inconsistent with the half-metallic character or even high spin polarization predicted for CrO_2 .^{2–6} The recognition

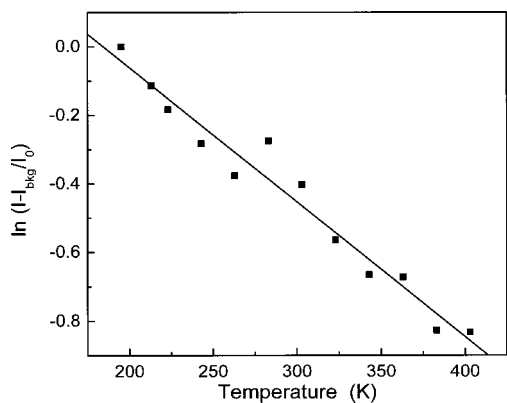


FIG. 4. The logarithm of XPS intensity of Cr $2p_{3/2}$ core level vs temperature. The fit expected for an effective Debye temperature of 370 K is shown.

that the surfaces of CrO_2 films are Cr_2O_3 (Ref. 16) does much to explain the very low density of states near the Fermi energy in the spin-polarized photoemission measurements,¹¹ but fails to explain the high polarization asymmetry observed in spin-polarized photoemission.¹¹ Induced polarization of the thin Cr_2O_3 surface layer, perhaps enhanced by defects, is clearly necessary to explain values of polarization approaching 90% to 100% reported in spin-polarized photoemission,¹¹ that in hindsight may be dominated by a Cr_2O_3 surface layer. While the x-ray diffraction results presented herein and elsewhere²³ suggest that the Cr_2O_3 surface layer is the anti-ferromagnetic corundum structure, the gamma, or cubic spinel structures of Cr_2O_3 that can show considerable stability at the surface,²⁴ can not be excluded as the dominant structure, and might more easily polarize the generally more stable corundum structure. Such an explanation is consistent with the results presented here.

The effective surface Debye temperature of the Cr_2O_3 surface layer can be evaluated by XPS and other surface sensitive techniques such as low-energy electron diffraction and reflection high-energy electron diffraction.²⁵ In the absence of surface phase transition, it is assumed that the emerging electron-beam intensity depends exponentially upon the sample temperature and this dependence is applicable to core level XPS at normal emission angle. The intensity of the photoelectron peak can be written as

$$I = I_0 \exp[-2W(T)], \quad \text{with } 2W = \frac{3\hbar^2(\Delta k)^2 T}{mk_B \theta_D^2},$$

where W is the Debye–Waller factor, T is the sample temperature, $\hbar(\Delta k)$ is the electron momentum transfer, m is the mass of the scattering center, and θ_D is the effective surface Debye temperature. The effective Debye temperature can be evaluated from the slope of a plot of $\ln(I/I_0)$ as a function of sample temperature, as shown in Fig. 4. A linear background was subtracted from each spectrum and normalization with respect to the intensity at the lowest temperature (I_0). We find that the effective Debye temperature θ_D is about 370 K. While typical of a metal, this effective Debye temperature is rather low for an oxide insulator and might contribute to strong temperature effects in Coulomb blockade.¹⁸

We have investigated CrO_2 thin film surfaces by using both x-ray photoemission and inverse photoemission. Our data show a large band gap between valence and conduction

bands, which indicates that the surface of CrO_2 film is insulating, while the transport measurements show that bulk material is conducting. We identify Cr_2O_3 as a stable oxide surface on CrO_2 films with an effective surface Debye temperature of about 370 K for the Cr_2O_3 surface layer. From ARXPS data, we found that the thickness of this insulating Cr_2O_3 layer is two times the mean free path. The CrO_2 “bulk” may induce some polarization in the Cr_2O_3 surface layer.

The support of the NSF (DMR 98-02126), the NSF CAREER program (Grant No. DMR 98-74657), the Office of Naval Research, and the Nebraska Research Initiative are gratefully acknowledged.

- ¹J. B. Goodenough, in *Progress in Solid State Chemistry*, edited by H. Reiss (Pergamon, Oxford, 1971), Vol. 5, p. 145.
- ²H. van Lueken and R. A. de Groot, *Phys. Rev. B* **51**, 7176 (1995).
- ³K. Schwarz, *J. Phys. F: Met. Phys.* **16**, L211 (1986).
- ⁴S. Matar, G. Demazeau, J. Sticht, V. Eyert, and J. Kübler, *J. de Physique I* **2**, 315 (1992).
- ⁵M. A. Korotin, V. I. Anisimov, D. I. Khomskii, and G. A. Sawatzky, *Phys. Rev. Lett.* **80**, 4305 (1998).
- ⁶S. P. Lewis, P. B. Allen, and T. Sasaki, *Phys. Rev. B* **55**, 10253 (1997).
- ⁷H. Y. Hwang and S.-W. Cheong, *Science* **278**, 1607 (1997).
- ⁸K. Suzuki and P. M. Tedrow, *Phys. Rev. B* **58**, 11597 (1998); A. M. Bratkovsky, *Phys. Rev. B* **56**, 2344 (1997).
- ⁹S. S. Manoharan, D. Elefant, G. Reiss, and J. B. Goodenough, *Appl. Phys. Lett.* **72**, 984 (1998).
- ¹⁰A. Barry, J. M. D. Coey, and M. Viret, *J. Phys.: Condens. Matter* **12**, L173 (2000).
- ¹¹K. P. Kämper, W. Schmitt, G. Güntherodt, R. J. Gambino, and R. Ruf, *Phys. Rev. Lett.* **59**, 2788 (1987).
- ¹²R. Weisendanger, H.-J. Güntherodt, G. Güntherodt, R. J. Gambino, and R. Ruf, *Phys. Rev. Lett.* **65**, 247 (1990).
- ¹³R. J. Soulen, J. M. Byers, B. Nadgorny, T. Ambrose, S. F. Cheng, P. R. Broussard, C. T. Tanaka, J. Nowak, J. S. Moodera, A. Barry, and J. M. D. Coey, *Science* **282**, 85 (1998).
- ¹⁴R. J. Soulen, M. S. Osofsky, B. Nadgorny, T. Ambrose, P. Broussard, and S. F. Cheng, *J. Appl. Phys.* **85**, 4589 (1999).
- ¹⁵W. J. DeSisto, P. R. Broussard, T. F. Ambrose, B. E. Nadgorny, and M. S. Osofsky, *Appl. Phys. Lett.* **76**, 3789 (2000).
- ¹⁶J. Dai, J. Tang, H. Xu, L. Spinu, W. Wang, K.-Y. Wang, A. Kumbhar, M. Li, and U. Diebold, *Appl. Phys. Lett.* **77**, 2840 (2000).
- ¹⁷P. A. Dowben, Y.-G. Kim, S. Baral-Tosh, G. O. Ramseyer, C. Hwang, and M. Onellion, *J. Appl. Phys.* **67**, 5658 (1990); R. Cheng, C. N. Borca, and P. A. Dowben, *Mater. Res. Soc. Symp. Proc.* **614**, F10.4.1 (2000).
- ¹⁸A. Sokolov, C.-S. Yang, L. Yuan, S.-H. Liou, R. Cheng, B. Xu, C. N. Borca, P. A. Dowben and B. Doblin (unpublished).
- ¹⁹C. Battistoni, J. L. Dormann, D. Fiorani, E. Paparazzo, and S. Viticoli, *Solid State Commun.* **39**, 581 (1981).
- ²⁰I. Ikemoto, K. Ishii, S. Kinoshita, H. Kuroda, M. A. A. Franco, and J. Thomas, *J. Solid State Chem.* **17**, 425 (1976).
- ²¹J. Choi, J. Zhang, S.-H. Liou, P. A. Dowben, and E. W. Plummer, *Phys. Rev. B* **59**, 13453 (1999); H. Dulli, E. W. Plummer, P. A. Dowben, Jaewu Choi, and S.-H. Liou, *Appl. Phys. Lett.* **77**, 570 (2000); Hani Dulli, P. A. Dowben, S.-H. Liou, and E. W. Plummer, *Phys. Rev. B* **62**, R14629 (2000); C. N. Borca, Bo Xu, T. Komesu, H.-Ky. Jeong, M. T. Liu, S.-H. Liou, and P. A. Dowben, *Appl. Phys. Lett.* (submitted).
- ²²C. B. Stagaescu, X. Su, D. E. Eastman, K. N. Altmann, F. J. Himpsel, and A. Gupta, *Phys. Rev. B* **61**, R9233 (2000).
- ²³R.-H. Cheng, C. N. Borca, P. A. Dowben, S. Stadler, and Y. U. Idzerda, *Appl. Phys. Lett.* **78**, 521 (2001); J. Graham, *J. Phys. Chem. Solids* **17**, 18 (1960).
- ²⁴P. S. Robert, H. Geisler, C. A. Ventrice, J. van Ek, S. Chaturvedi, J. A. Rodriguez, M. Kuhn, and U. Diebold, *J. Vac. Sci. Technol. A* **16**, 990 (1998).
- ²⁵C. Waldfried, D. N. McIlroy, J. Zang, P. A. Dowben, G. A. Katrich, and E. W. Plummer, *Surf. Sci.* **363**, 296 (1996); C. N. Borca, D. Ristoiu, T. Komesu, H.-K. Jeong, C. Hordequin, J. Pierre, J. P. Nozieres, and P. A. Dowben, *Appl. Phys. Lett.* **77**, 88 (2000).